Strength of Materials, Vol. 39, No. 5, 2007

ASSESSMENT OF MECHANICAL PROPERTIES AND PHASE-STRUCTURAL STATE IN CORROSION-RESISTANT STEELS UNDER STATIC AND LOW-CYCLE LOADING

V. I. Vitvitskii, V. I. Tkachev, M. F. Berezhnitskaya, and R. V. Chepil'

UDC 620.1975

The use of an austenite stability factor provides (calculated from chromium and nickel equivalents) a quantitative assessment of phase-structural state in corrosive-resistant steels by their chemical composition. Based on the austenite stability factors, a correlation has been established between mechanical properties of the steels under static loading. The low-cycle fatigue life is proposed to be determined from the chemical composition and specimen contraction.

Keywords: corrosion-resistant steels, mechanical properties, low-cycle fatigue life, austenite stability factor.

Introduction. For the development of structural materials, researchers should know quantitative relationships between chemical composition, structure and mechanical properties of alloys. The definition and practical application of the relationships is one of important and first-priority tasks in materials science. As for now, metallic materials and related processes are developed by using expensive empirical approaches. The applicability of the available quantitative relationships is limited to narrow ranges of compositions, structures, and properties. In the case of corrosion-resistant materials, the above-mentioned correlation has been established for low-strength austenitic steels only [1]. Also, some equations have been derived to relate the indices of static and low-cycle loading [2, 3], but there some limitations on their applicability because the discrepancy between experimental and calculated data may be rather significant [3]. Furthermore, the interrelation between static mechanical properties has not been studied properly. The main drawback of the available approaches is that they do not involve any quantitative index that would allow for the phase-structural state in materials based on their chemical composition.

The objective of the present study has been to define, for corrosion-resistant chromium and chromium-nickel steels as an example, an index that would represent phase-structural state in material and to assess its applicability for the determination of a relation between strength and plasticity characteristics as well as between properties of material under static and low-cycle loading.

Investigation Procedure and Results. *Definition of a Phase-Structural Index.* The main factor that dictates the deformation behavior and service characteristics (ultimate strength σ_b, yield stress $\sigma_{0.2}$, plastic limits δ, ψ, and low-cycle fatigue life N) of a particular material is the bcc or fcc structure. For ternary Fe–Cr–Ni alloys, it is defined from an appropriate equilibrium diagram (Fig. 1) which shows the phase state of steel depending on the chromium and nickel content. For alloys with larger amounts of alloying elements, chromium and nickel equivalents (*CrE* and *NiE*) are used instead of Ni and Cr according to Sheffler and Schneider [1]. These equivalents are calculated by the well-known expressions

$$CrE = [\mathrm{Cr}] + 2[\mathrm{Si}] + 1.5[\mathrm{Mo}] + 5[\mathrm{V}] + 5.5[\mathrm{Al}] + 1.75[\mathrm{Nb}] + 1.5[\mathrm{Ti}] + 0.75[\mathrm{W}], \quad (1)$$

$$NiE = [\mathrm{Ni}] + [\mathrm{Co}] + 0.5[\mathrm{Mn}] + 0.3[\mathrm{Cu}] + 25[\mathrm{N}] + 30[\mathrm{C}], \quad (2)$$

where the content of the elements in wt.% is shown in square brackets.

Karpenko Physicomechanical Institute, National Academy of Sciences of Ukraine, Lvov, Ukraine. Translated from Problemy Prochnosti, No. 5, pp. 19 – 30, September – October, 2007. Original article submitted March 1, 2006.

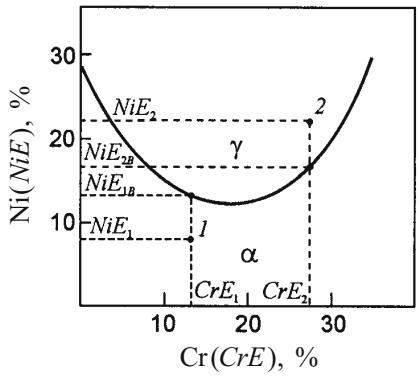

Fig. 1. Variation of phase state in ternary Fe–Cr–Ni alloys as a function of the amount of Cr(*CrE*) and Ni(*NiE*): (*1*, *2*) determination of NiE_{1B} and NiE_{2B} in the alloys with the coordinates *CrE*, *NiE*, Cr_2E, and Ni_2E, the parabola corresponds to the minimum *NiE* values sufficient for producing 100% austenite, γ – austenite, and α – ferrite or transitional structures.

According to these relationships, the influence of 14 elements is reduced to two equivalents (*CrE* and *NiE*). Based on them, a phase-structural index was defined. In so doing, we assumed that the location of the phase curve in Fig. 1 was not a structural index. Furthermore, the location of the phase curve in Fig. 1 was assumed to remain unaffected by substitution of *CrE* and *NiE* for Cr and Ni and to be described by a parabola,

$$(NiE)_B = 0.0512\,(CrE)^2 - 1.843\,(CrE) + 28.6. \qquad (3)$$

The material's phase state and thus its deformation mechanism and properties depend on where the point with the phase state coordinates lies relative to the concentration curve that separates the γ and α regions. For each particular alloy with its peculiar chemical composition, we determined the actual chromium and nickel equivalents by expressions (1) and (2). Then, using Eq. (3) we calculated the basic nickel equivalent $(NiE)_B$ corresponding to the particular value of the chromium equivalent on the parabola and compared it to the actual nickel equivalent of the alloy. From the above reasoning, it is proposed to characterize a material using an austenite stability factor $A_\gamma = (NiE)/(NiE)_B$ that shows the extent to which the actual equivalent is higher or lower than the basic one. In essence, the factor A_γ is a quantitative measure of the excess or deficiency of austenite formers in this material to produce 100% austenite.

Table 1 summarizes the A_γ values for some corrosion-resistant steels of the main structural classes. The factor A_γ ranges from 0.15 to 0.44 for ferritic structures, from 0.55 to 0.71 for martensitic ones, and from 0.72 to 0.96 for transitional structures. If $A_\gamma \approx 1$, the chemical composition coincides with the minimum sufficient amount of elements for the formation of a fully austenitic structure, e.g., a carbon-free steel 00Kh18N12. Stability of this austenite is easily disturbed by any additional strain or thermal effects. By these we mean the $\gamma \to \alpha$ strain transformations of various kinetics in Cr–Ni and Cr–Ni–Mn steels, low-temperature phase transitions, etc. If $A_\gamma > 1$, the γ phase is stable over a wide range of operating conditions, with the following features inherent in the fcc lattice: plastic relaxation reserves, stacking-fault energy, age-hardening ability, which govern the high-temperature, corrosion-resistant and mechanical properties, etc. In general, the data in Table 1 show that A_γ varies symbatically with the nickel equivalent of materials: to an increase in the austenite-forming ability of the chemical compositions there corresponds a growth of the austenite stability factor and formation of the related phase-structural states.

Strength and Plasticity. Mechanical properties (σ_b, $\sigma_{0.2}$, δ, and ψ) of steels were determined through static tensile testing of five-fold smooth specimens 5 mm in diameter at 293 K, with a constant head speed of 0.1 mm/min, on a Mod. UMÉ-10TM testing machine. The total ranges of the parameters studied were the following: σ_b = 380–1340 MPa, $\sigma_{0.2}$ = 200–1100 MPa, δ = 12–72%, and ψ = 24–83% (Table 1). Steels 1Kh13, 2Kh13, 1Kh12N2VMFBA, 15Kh16N2M, 1Kh18N10T, 04Kh11N43M2T are presented upon various heat treatment operations.

TABLE 1. Materials under Study and Their Characteristics

No.	Material, heat treatment temperature and time, and quenching medium	Structure	*CrE*	*NiE*	A_γ	σ_b, MPa	$\sigma_{0.2}$, MPa	δ, %	ψ, %	Reference
1	2	3	4	5	6	7	8	9	10	11
1	08Kh17E, T = 1053 K, water	F	20.84	1.90	0.153	460 404	260	37.0 37.0	66.0 72.0	–
2	1Kh13(II)	F	14.60	4.40	0.349	620 573	390	25.8 27.0	67.3 71.0	[2]
3	1Kh13(I), T = 1273 K, 120 min, air; T = 1033 K, 120 min, air	F	14.60	4.40	0.349	638 701	429	35.0 29.0	77.0 77.0	[2]
4	Kh25N6M	F	29.00	8.00	0.439	620 676	380	28.0 32.0	57.0 62.0	–
5	1Kh17N2Sh, T = 1263 K, 120 min, oil; T = 823 K, 120 min, water	M + F	18.20	6.60	0.549	912 840	707	16.9 19.0	55.0 48.0	[2]
6	2Kh13, T = 1323 K	M	13.20	7.30	0.553	1000 1025	850	17.0 18.0	65.0 59.0	[4]
7	2Kh13, T = 1323, 843 K	M	13.20	7.30	0.553	1215 1287	1080	16.0 13.0	68.0 63.0	[4]
8	15Kh16N2M, T = 1313, 933 K	M	17.80	6.80	0.566	980 962	800	18.0 17.0	41.0 55.0	[4]
9	15Kh16N2M, T = 1313, 843 K	M + C	17.80	17.80	0.566	1200 1063	900	12.0 18.0	50.0 54.0	[4]
10	1Kh12N2VMF, T = 1293, 1033 K	M + C	14.85	14.85	0.635	970 1051	865	18.5 16.0	59.5 63.0	–
11	1Kh12N2VMFBA, T = 1293, 933 K	M + C + I	15.73	8.75	0.710	1105 1125	970	17.5 16.0	59.0 60.0	[4]
12	1Kh12N2VMFBA, T = 1293, 873 K	M + C + I	15.73	8.75	0.710	1340 1244	1115	14.5 17.0	64.5 71.0	–
13	20Kh14N3M2B, T = 1383 K, oil; T = 923 K, 120 min, air	A + M + C	17.20	8.70	0.722	1000 961	790	17.0 17.0	65.0 60.0	–
14	02Kh11N11MF, T = 1223 K, 15 min, 523 K	A_{min} + M + I_{min}	15.78	9.80	0.799	1000 1075	950	17.0 16.0	75.0 64.0	–
15	02Kh10N9T2M2	A + M	16.66	10.55	0.871	1110 1092	1010	20.0 18.0	64.0 68.0	[2]
16	03Kh12N9MT, T = 1273 K, 60 min, 823 K	A + M + I_{min}	14.34	11.86	0.933	1050 1025	950	17.0 19.0	60.0 61.0	–
17	03Kh10N8K4MFD	A + M + I	12.05	13.29	0.961	1100 1104	1070	18.0 18.0	65.0 62.0	–
18	Kh5CrNi 18-12 (like 05Kh19N10), T = 1323 K, water	A + M_s	18.80	12.10	1.004	600 520	200	72.0 83.0	50.0 53.0	[5]
19	1Kh18N10T, T = 1423, 1023 K, 600 min	A + M_s	19.20	12.70	1.051	650 638	250	71.0 72.0	53.6 65.0	[2]
20	1Kh18N10T, T = 1323 K, water	A + M_s	20.18	13.00	1.060	660 723	290	67.0 64.0	62.0 75.0	–
21	08Kh18N10 (0.022% N), T = 1323 K, water	A + M_s	18.00	12.95	1.078	590 577	224	78.0 73.0	74.0 59.0	[6]
22	03Kh13AG19, T = 1273 K, water	A	14.70	13.95	1.110	890 848	381	63.0 66.0	74.5 68.0	–
23	Kh2CrNiMo 18-12 (like 08Kh18N14M2), T = 1323 K, water	A	21.73	15.30	1.202	600 626	250	68.0 65.0	83.0 64.0	[5]
24	08Kh18N10 (0.26% N), T = 1323 K, water	A	18.00	18.90	1.573	785 837	433	56.0 53.0	70.0 74.0	[6]
25	06Kh12G20AN5, T = 1273 K, water	A	15.50	20.25	1.642	800 809	420	54.0 55.0	62.0 70.0	–
26	00Kh19N23V2T, T = 1323 K, water	A	23.22	22.80	1.700	550 526	220	48.0 50.0	50.0 51.0	–

continued Table 1

1	2	3	4	5	6	7	8	9	10	11
27	06Kh27N16G6A, T = 1323 K, water	A	28.67	31.00	1.737	810 851	470	52.0 50.0	66.0 75.0	–
28	04Kh12N36Yu3TV, T = 1023 K, 120 min; 923 K, 240 min	A + I	30.78	37.95	1.862	1110 1115	820	31.0 31.0	51.0 50.0	–
29	03Kh21N32M3B, T = 1613 K, 120 min	A	28.40	33.89	1.931	640 642	330	41.0 39.0	70.0 72.0	–
30	06Kh20N16AG6, T = 1323 K, water	A	21.20	24.30	1.938	780 750	410	52.0 54.0	75.0 62.0	–
31	06Kh14G20AN10M, T = 1273 K, water	A	19.35	29.60	2.445	810 767	460	48.0 44.0	70.0 50.0	–
32	03Kh11N43M2T, T = 1323 K, 120 min, air cooling; 1003 K, 900 min; 963 K, 60 min	A + I	28.34	44.09	2.520	1180 1153	770	21.0 41.0	24.0 34.0	–
33	04Kh11N43M2T, No. 32 + T = 1473 K, cooled to 1273 K, 120 min, air	A + I_{min}	28.34	44.09	2.520	815 838	505	37.0 25.0	38.0 51.0	–
34	04Kh11N43M2T, No. 32 + T = 1473 K, cooled to 1273 K, 120 min; 1023 K, 480 min; 923 K, 480 min, air	A + I	28.34	44.09	2.520	1250 1270	820	29.0 25.0	49.0 35.0	–

Notes: 1. The experimental and calculated data are given above and under the line, respectively. 2. A – austenite, F – ferrite, M – martensite; M_s – strain-induced martensite; C – carbides; I – intermetallides.

A study of the relation between strength and yield stress shows it to be of qualitative nature: materials with almost equal yield stress $\sigma_{0.2}$ may differ in σ_b and A_γ (Fig. 2a). This renders their quantitative assessment impossible. If the austenite stability index A_γ is added to the main characteristics, the materials can be arranged in a certain order and the appropriate quantitative relationships can be established. Here, the sought-for expression is written as $A_\gamma^m a^n = f(A_\gamma^k b^p)$, where a and b are the indices of the mechanical properties. The function f was determined graphically in the coordinates $Y = A_\gamma^m a^n$, $X = A_\gamma^k b^p$. The coordinates and the curve were optimized through iteration of m, n, k, and p, so that the approximation equation had the correlation coefficient $R > 0.95$. The outcome of approximation was considered acceptable if the difference between the actual and calculated values did not exceed the error of experimental results. To plot the relationship between the strength indices we used the coordinates $A_\gamma^m \sigma_b^n - A_\gamma^k \sigma_{0.2}^p$. Following the above procedures and calculations, a diagram of $\sqrt{A_\gamma \sigma_b}$ vs. $\sqrt{A_\gamma \sigma_{0.2}}$ was plotted (Fig. 2b); based on these functions, we obtained four approximation equations (Table 2), each corresponding to a definite range of $\sigma_{0.2}$:

Group I (the lowest strength, 200 MPa $\le \sigma_{0.2} \le$ 330 MPa): materials in the homogeneous state of a single-phase solution of substitution, with A_γ ranging from 0.152 to 2.52, namely, steels Kh5CrNi 18-12, 00Kh19N23V2T, Kh2CrNiMo 18-12, 08Kh18N10 (0.022% Ni), 1Kh18N10T, 08Kh17T, and 03Kh21N32M3B (quenched).

Group II (380 MPa $\le \sigma_{0.2} \le$ 600 MPa): materials alloyed with substitution elements and strengthened by soluble nitrogen as an interstitial element, namely, steels 1Kh13 (upon high-temperature tempering), Kh25N6M, 03Kh13AG19, 06Kh12G20AN5, 06Kh27N16AG6, 06Kh14G20AN10M, and 08Kh18N10 (0.26% N) and quenched alloy 03Kh11N43M2T.

Materials in the heterogeneous (multiphase) state were included into the following two high-strength groups:

Group III (770 MPa $\le \sigma_{0.2} \le$ 890 MPa): economically alloyed corrosion-resistant Fe–Ni alloys with a moderate (10–20%) amount of strengthening phases, such as 04Kh12N36Yu8TV, 04Kh11N43M2T upon ageing and overageing, 03Kh21N32MZB; steels with carbide and intermetallic strengthening 2Kh13, 20Kh14N3M2B; 1Kh17N2Sh, 1Kh12N2VMF, 15Kh16N2M.

TABLE 2. Results of Approximation of Relationships between Strength and Plasticity Indices for Corrosion-Resistant Steels, Allowing for A_γ

Strength group	Parameter	Approximation equation	Correlation coefficient R	Mean error, %
	σ_b	$y = \sqrt{A_\gamma \sigma_b}$; $x = \sqrt{A_\gamma \sigma_{0.2}}$		
I		$y = -7.9091 + 2.7649x - 0.0419x^2$	0.9925	7.3
II		$y = -36.82036 + 6.3743x - 0.20032x^2 + 0.00243x^3$	0.9974	5.7
III		$y = -10.50464 + 2.29781x - 0.0466x^2 + 6.27 \cdot 10^{-4} x^3$	0.9918	3.6
IV		$y = -93.33867 + 11.77788x - 0.39621x^2 + 0.00473x^3$	0.9818	4.8
	δ	$y = A_\gamma \sqrt{\delta}$; $x = A_\gamma \sqrt{\sigma_b / \sigma_{0.2}}$ (σ_b – calculated)		
I		$y = 0.0016 + 0.4216x + 0.1507x^2 - 0.0523x^3$	0.9955	5.4
II		$y = 0.0067 + 0.345x + 0.1718x^2 - 0.0385x^3$	0.9974	8.7
III		$y = 0.223 - 0.2666x + 0.5366x^2 - 0.1106x^3$	0.9938	8.3
IV		$y = 0.0015 + 0.2249x + 0.1917x^2$	0.9582	14.7
	ψ	$y = A_\gamma^2 \sqrt{\psi}$; $x = A_\gamma^2 \sqrt{\sigma_{0.2}/E}$		
I		$y = 0.3233 - 1.1932 \log x - 0.99506(\log x)^2 - 0.14006(\log x)^3$	0.9986	12.8
II		$y = 0.55021 - 0.91735 \log x - 0.97544(\log x)^2 - 0.16003(\log x)^3$	0.9984	13.2
III		$y = 0.8529 - 0.0638 \log x - 0.47625(\log x)^2 - 0.06397(\log x)^3$	0.9965	17.8
IV		$y = -23.0781 - 37.3783 \log x - 19.8295(\log x)^2 - 3.39705(\log x)^3$	0.9960	6.7

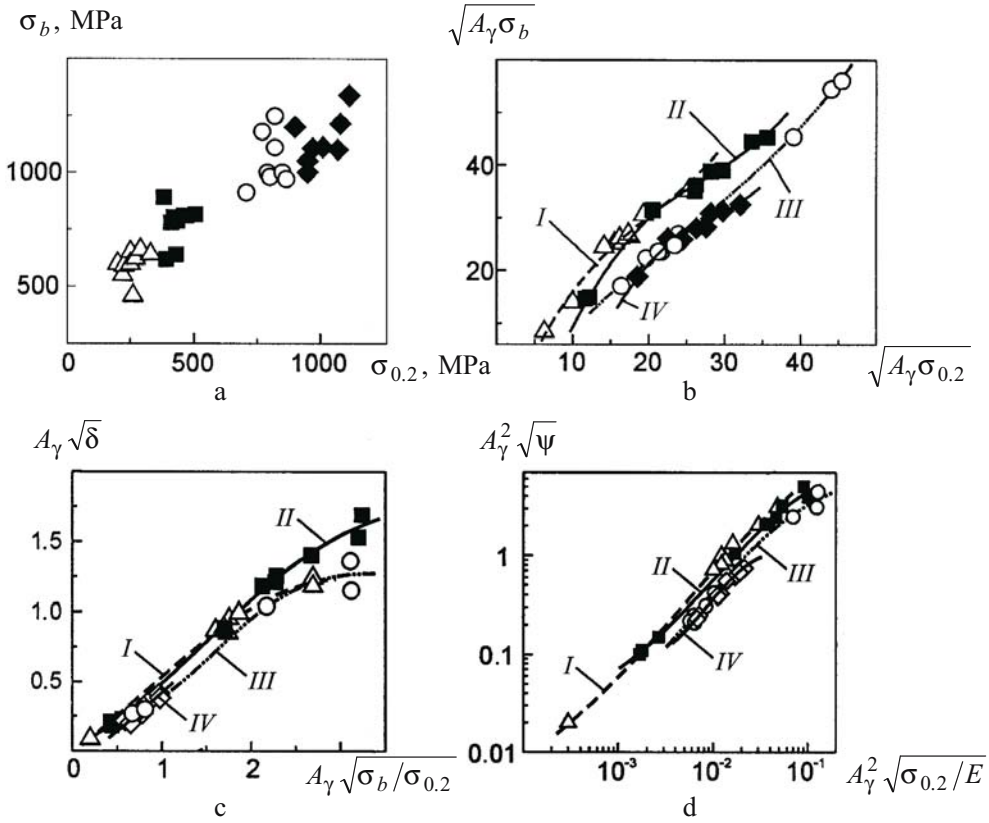

Fig. 2. Graphical representation of the relationships between strength and plasticity indices of steels, allowing for A_γ (b–d) and without A_γ (a). (Figures *I*, *II*, *III*, *IV* denote the respective strength groups.)

Group IV ($\sigma_{0.2} \geq 900$ MPa): complex-alloyed steels 2Kh13, 1Kh12N2VMFBA (two heat treatment operations) and low-carbon martensite-ageing steels 02Kh11N11MF, 03Kh10N8K4MFD, 03Kh12N9MT, 02Kh10N9T2M2.

Note that for Group I – the lowest-strength material – the greatest mean deviation of calculated σ_b values from the experimental ones is 7.3%, while for the other three groups – constructionally efficient alloys – it is less than 4–6% (Table 2).

Analysis of the experimental data demonstrates that as the strength margin increases, so does δ. The hardening coefficient is known to be defined by the ratio $\sigma_b/\sigma_{0.2}$ or $1-\sigma_{0.2}/\sigma_b$ [1–3]. Here, for each group of materials the relationship between the hardening coefficient and specific elongation is approximated by a separate curve in the coordinates $A_\gamma\sqrt{\delta} - A_\gamma\sqrt{\sigma_b/\sigma_{0.2}}$ (Fig. 2c, Table 2), while that between the hardening coefficient and specific reduction of area in the coordinates $A_\gamma^2\sqrt{\psi} - A_\gamma^2\sqrt{\sigma_{0.2}/E}$ (Fig. 2d, Table 2). The modulus of elongation $E = 2\cdot10^5$ MPa.

Low-Cycle Fatigue. Flat specimens 2–3 mm thick made of steels Nos. 1, 13, 14, 16, 17, 25–28, 32–34 (Table 1) were subjected to low-cycle pure bending loading with pulsating strain cycles in air on a Mod. IP-2VTD test machine by the procedure [7]. The cycling frequency was 0.5 Hz and the test temperature was 293 K. The strain cycle amplitude ε was 0.8, 1.2, and 1.6%, the test base was varied from $5\cdot10^2$ to $5\cdot10^4$ cycle. The influence of heat treatment on the low-cycle fatigue was studied for steel 03Kh11N43M2T. The test results are summarized in Table 3.

The low-cycle strength under severe loading is usually calculated by Coffin–Manson equations $\varepsilon N^k = C$. The k and C values vary from publication to publication as follows: $k = 0.4$–0.6 and $C = (0.5\text{–}1.2)e_f$ (e_f is the effective elongation to fracture) or $C = 1/2\ln[1/(1-\psi)]$ [3, 5]. The difference between the experimental and calculated values of the number of cycles to failure according to these equations is as large as 5–10-fold. A comparison (Tables 1 and 3) of behavior of deformation characteristics δ and ψ and the low-cycle fatigue life N of the materials has demonstrated that of all the static loading indices the specific reduction of area (contaction) ψ is the most sensitive one. However, this correlation is limited to the groups of materials that are in similar phase-structural states. For the materials which have the same ψ but differ in structure, the difference in fatigue life can be significant. For example, for a ferritic steel 08Kh17T and austenitic steel 06Kh26NAG6 we have $\psi = 66\%$ and the fatigue life at $\varepsilon = 1.6\%$ is 800 and 4000 cycles, respectively; i.e., the solely deformational statement, when applied to corrosion-resistant steels, gives considerable errors. To allow for the phase-structural state quantitatively, we used A_γ. In the general form, the analytical expression is written as $A_\gamma^m N^n = f(A_\gamma^k \psi^p)$. A specific solution was sought for by following the algorithm outlined above, for each strain cycle amplitude. Figure 3 shows the relationship $A_\gamma^2\sqrt{N} - A_\gamma^2\sqrt{\psi}$ for various strain amplitudes. To minimize the gap between the experimental and calculated data, the behavior of transitional structures with $A_\gamma < 1$ and austenitic materials with $A_\gamma \geq 1$ was described by separate relationships (Table 4). We plotted a diagram in the coordinates $Y = (A_\gamma\varepsilon)^l\sqrt{N}$, $X = A_\gamma^2\sqrt{\psi}$ and determined $l = 3/2$ (Fig. 4) in order to establish a relation between the strain cycle amplitude and life. Each expression in Table 4 represents a relation between the properties of materials under static and fatigue loading, over a wide range of strength (200 MPa $\leq \sigma_{0.2} \leq$ 1000 MPa). The life values calculated by formulas (1)–(3), (5)–(7), (4) and (8) (Table 4) are summarized in Table 3.

Discussion. It has been found that one needs only a single index A_γ of the γ-phase activity of elements of a material's chemical composition in order to establish a correlation between mechanical properties, with $R > 0.95$, for the alloys within the strength range 200 MPa $\leq \sigma_{0.2} \leq$ 1115 MPa. Materials can be assigned to various strength groups depending on the heat treatment. In particular, the as-quenched alloy 04Kh11N43M2T belongs to group II, while the same alloy upon ageing falls into group III. Heat treatment results in structural alterations, which brings steels 15Kh16N2M, 2Kh13, 1Kh12NV2MF from group III to group IV. Alloying has a similar effect. Steel 08Kh18N10 with 0.022% N qualifies as group I but belongs to group II when its nitrogen content is 0.26%. The migration of the materials from one group to the other is accompanied by a corresponding change in the relationships between their properties as described by the equations in Table 2.

TABLE 3. Experimental and Calculated Values of Low-Cycle Fatigue Life for Corrosion-Resistant Steels

Material No. as per Table 1	Low-cycle fatigue life N (cycle) at strain amplitude ε (%)		
	0.8	1.2	1.6
1	–	–	$\frac{800}{800}$ (925)
13	$\frac{9000}{9000}$ (7100)	$\frac{3100}{3100}$ (2100)	$\frac{1000}{1000}$ (890)
14	$\frac{15800}{15800}$ (12000)	$\frac{4200}{4200}$ (3560)	$\frac{1300}{1300}$ (1500)
16	$\frac{26300}{26300}$ (15330)	$\frac{5300}{5300}$ (4540)	$\frac{2100}{2100}$ (1920)
17	$\frac{17000}{16250}$ (14950)	$\frac{4300}{4470}$ (4430)	$\frac{1700}{1470}$ (1870)
20	$\frac{12000}{11970}$ (13080)	$\frac{3000}{3000}$ (3870)	$\frac{1800}{2015}$ (1630)
25	$\frac{27000}{28410}$ (22290)	$\frac{8000}{7870}$ (6600)	$\frac{2600}{2560}$ (2790)
26	$\frac{20500}{23010}$ (19080)	$\frac{5700}{6350}$ (5650)	$\frac{1850}{2110}$ (2380)
27	$\frac{28000}{31970}$ (25300)	$\frac{8700}{8420}$ (7495)	$\frac{4000}{3550}$ (3160)
28	$\frac{28000}{24740}$ (20900)	$\frac{6300}{6510}$ (6190)	$\frac{2750}{2760}$ (2610)
32	$\frac{27500}{27500}$ (27945)	$\frac{4900}{4900}$ (8200)	$\frac{2500}{2510}$ (3490)
33	$\frac{21700}{20820}$ (21520)	$\frac{4700}{4170}$ (6370)	$\frac{2660}{2620}$ (2690)
34	$\frac{11600}{12180}$ (13160)	$\frac{2800}{2885}$ (3900)	$\frac{1590}{1660}$ (1645)

Note. The figure above and below the line are, respectively, the experimental data and the data calculated by formulas (1)–(3), (5)–(7) in Table 4; the values found by formulas (4) and (8) in Table 4 are in brackets.

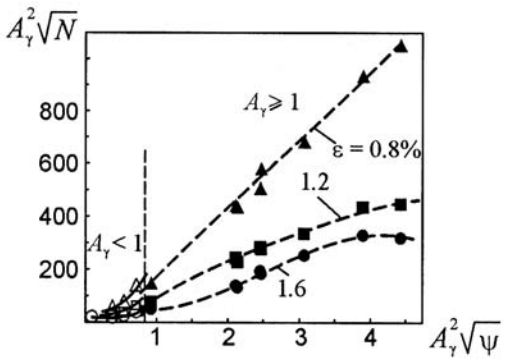

Fig. 3

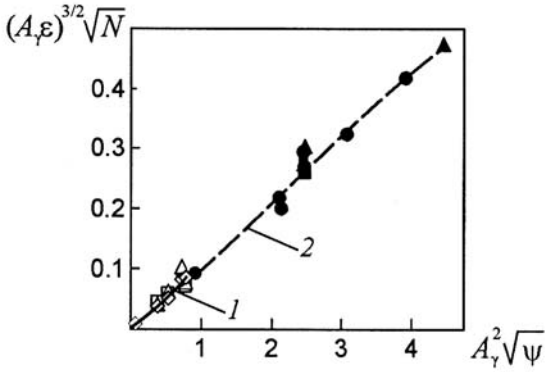

Fig. 4

Fig. 3. Relationship between life N and specific elongation ψ, allowing for A_γ for the strain cycle amplitudes ε.
Fig. 4. Relationship between strain ε and life N: (*1*) $A_\gamma < 1$; (*2*) $A_\gamma \geq 1$.

Introducing the parameter A_γ has enabled us to find relationships between indices of static and low-cycle loading; with these expressions the mean deviation of calculated values from experimental ones does not exceed 9.6% (equations (1)–(3) and (5)–(7), Table 4) and 13.9–20.0% (equations (4) and (8), Table 4). This improvement in prediction accuracy by considering the phase-structural state of materials will in future make it possible to decrease safety factors in the low-cycle strength calculations, and thus reduce the steel intensity and cost of final products.

TABLE 4. Results of Approximation of Relationships between Specific Elongation and Low-Cycle Fatigue Life for Corrosion-Resistant Steels, Allowing for A_γ

A_γ	Formula No.	Parameter	Approximation equation	Correlation coefficient, R	Mean error, %
< 1		N	$y = A_\gamma^2\sqrt{N}$; $x = A_\gamma^2\sqrt{\psi}$		
	(1)		$\varepsilon = 1.6\%$: $y = -1.1369 + 99.659x - 232.16x^2 + 238.11x^3$	1.0000	0
	(2)		$\varepsilon = 1.2\%$: $y = 30.175 - 58.645x + 143.66x^2$	1.0000	0
	(3)		$\varepsilon = 0.8\%$: $y = 68.928 - 221.33x + 442.1x^2$	1.0000	0
			$y = (A_\gamma\varepsilon)^{3/2}\sqrt{N}$; $x = A_\gamma^2\sqrt{\psi}$		
	(4)		$y = 0.0023 + 0.0709x + 0.0494x^2$	0.9960	20.0
≥ 1			$y = A_\gamma^2\sqrt{N}$; $x = A_\gamma^2\sqrt{\psi}$		
	(5)		$\varepsilon = 1.6\%$: $y = 121.6 - 187.15x + 127.69x^2 - 17.01x^3$	0.9985	9.6
	(6)		$\varepsilon = 1.2\%$: $y = -74.699 + 176.23x - 13.37x^2$	0.9990	4.2
	(7)		$\varepsilon = 0.8\%$: $y = -91.316 + 256.92x + 0.1217x^2$	0.9982	6.3
			$y = (A_\gamma\varepsilon)^{3/2}\sqrt{N}$; $x = A_\gamma^2\sqrt{\psi}$		
	(8)		$y = -0.0003 + 0.1046x + 0.0007x^2$	0.9851	13.9

In general, by monitoring the values of m and k in expressions $A_\gamma^m a^n = f(A_\gamma^k b^p)$ we can trace the influence of structural factor on the relations between force, strain and fatigue characteristics; in particular, the parameters m and k are 0.5 in the strength assessment (σ_b, $\sigma_{0.2}$), equal to 1 in the calculation of specific elongation (δ), and 2 in the cases of reduction of area (ψ) and life (N).

The result can be helpful for nondestructive testing of the materials that tend to change their properties over the operation period. Using the proposed procedure, the mechanical properties of a metal at its heterogeneous areas can be calculated from a single strength characteristic (e.g., by measuring hardness and then determining σ_b from it) without any significant damage to the metal integrity.

This approach can be useful for improving the reliability of life assessment for structural materials over a wide range of operating conditions, where the material structure is a critical factor: under various loading conditions, temperatures, liquid and gaseous media, including high-pressure service, in the presence of stress raisers, etc.

CONCLUSIONS

1. The phase-structural state of corrosion-resistant chromium and chromium-nickel steels is proposed to be quantitatively allowed for by means of the austenite stability factor A_γ.

2. The use of the factor A_γ makes it possible to determine σ_b, δ, and ψ from experimental values of $\sigma_{0.2}$ over the interval 200 MPa $\le \sigma_{0.2} \le$ 1115 MPa and chemical composition of steels and to calculate the low-cycle fatigue life from the chemical composition and specific reduction of area, with peculiar relationships for the materials with $A_\gamma < 1$ (steels of transitional class) and $A_\gamma \ge 1$ (austenitic steels).

REFERENCES

1. F. B. Pickering, *Physical Metallurgy and the Design of Steels* [Russian translation], Metallurgiya, Moscow (1982).
2. V. T. Troshchenko, *Deformation and Fracture in Metals under High-Cycle Loading* [in Russian], Naukova Dumka, Kiev (1981).

3. N. A. Makhutov, A. Z. Vorob'ev, M. M. Gadenin, et al., *Low-Cycle Strength of Structures* [in Russian], Nauka, Moscow (1983).
4. T. N. Kalichak, *Investigation of Some Physical-Mechanical and Electrochemical Properties of Martensitic Stainless Steels* [in Russian], Author's Abstract of the Candidate Degree Thesis (Tech. Sci.), Kiev (1971).
5. W. Dahl and P. Belche, "Stress–strain diagram," in: W. Dahl and W. Anton (Eds.), *Static Strength and Fracture Mechanics of Steels* [Russian translation], Metallurgiya, Moscow (1986), pp. 51–133.
6. M. E. Pridantsev, N. P. Talov, and F. L. Levin, *High-Strength Austenitic Steels* [in Russian], Metallurgiya, Moscow (1969).
7. V. I. Tkachev, V. I. Kholodnyi, and I. N. Levina, *Performance of Steels and Alloys in Hydrogen Service* [in Russian], Vertikal', Lvov (1999).